

Synthesis and characterization of thin amorphous carbon films doped with nitrogen on (001) Si substrates

I Balchev¹, Kr Tzvetkova¹, S Kolev¹, P Terziiska², A Szekeres², I Miloushev², T Tenev², K Antonova², R Peyeva², T Ivanova³, I Avramova⁴, M Tzvetkov⁵, G Avdreev⁵, E Valcheva⁶, T Milenov¹ and S Tinchev¹

¹Institute of Electronics- Bulgarian Academy of Sciences, 72 Tzarigradsko Shausee Blvd., 1784 Sofia, Bulgaria

²Institute of Solid State Physics- Bulgarian Academy of Sciences, 72 Tzarigradsko Shausee Blvd., 1784 Sofia, Bulgaria

³Central Laboratory of Solar Energy and New Energy Sources- Bulgarian Academy of Sciences, 1784 Sofia, Bulgaria

⁴Institute of General and Inorganic Chemistry, Bulgarian Academy of Sciences, Acad. G. Bonchev Str., bl. 11, 1113 Sofia, Bulgaria

⁵"R. Kaishev" Institute of Physical Chemistry, Bulgarian Academy of Sciences, Acad. G. Bonchev Str., bl. 11, 1113 Sofia, Bulgaria

⁶Faculty of Physics, Sofia University, 5 James Bourchier Blvd., 1164 Sofia, Bulgaria

E-mail: ivobalchev@gmail.com

Abstract. We synthesized undoped as well as up to 6 at.% nitrogen (N) doped thin amorphous carbon (α -C) films by plasma- enhanced chemical vapor deposition (PECVD) method. The source of carbon/carbon containing radicals was benzene (C_6H_6) in Ar gas- mixture. The obtained thin films were studied by optical microscopy, X-ray powder diffraction, UV-VIS-NIR Spectral Ellipsometry, IR and Raman spectroscopic studies as well as by X-ray photoelectron spectroscopies (XPS). We established by XPS that the deposited layers consist of a mix of sp^2 and sp^3 hybridized carbon. The films are amorphous as it was shown by the measured XRD patterns. The ellipsometric measurements enabled calculation of transition energies and the complex results showed that films with thickness of 15- 120 nm and different properties can be obtained by this technique.

1. Introduction

Over the last decades carbon-based materials and α -C (sp^2 - dominated amorphous carbon films) and ta-C(sp^3 dominated diamond-like carbon films) especially are extensively investigated for use in electronic applications. The plasma enhanced chemical vapor deposition (PECVD) method is the most widely used due to its high reliability, relatively low cost etc. It is established that the optical bandgap E_g of the deposited films can be easily varied with the plasma voltage [1]. Additionally, the charge transport properties can be modified by doping. Nitrogen (N) looks perfect candidate as it has very similar size as carbon and belongs to III group of the Periodic system. Moreover, the nitrogen level in forbidden gap of ta-C is shallow [2]. Different carbon containing precursors are investigated but methane is the preferred one due its relatively high ionization potential and low deposition rate [3,4]. Conversely, the application of benzene as a precursor is usually avoided due to its low ionization potential and high deposition rate of about 2 nm/s or higher [5-7]. Moreover, the charge transport in this case is most probably governed by hopping conduction in the valence band tail [5].

We aimed in the deposition of N-doped hydrogenated carbon films with different sp^2/sp^3 ratio by PECVD at low deposition rates for application in gas-detectors. Here we present some preliminary results of characterization of several representative specimens of hydrogenated ta-C and α -C doped with 0.1- 1 at.% N.



2. Experimental

Hydrogenated ta-C (ta-C:H) and α -C (α -C:H) thin films were deposited in a DC plasma CVD reactor. We used benzene as a hydrocarbon precursor and an argon residual pressure. More information about the used process and equipment can be found in [1]. The Si substrates were placed on cathode while the metal vacuum chamber acted as anode. Benzene vapour was obtained in a thermostat at about 25°C. Before the film deposition the substrates were cleaned in acetone, ethanol and deionized water in ultrasonic bath followed by a 10 min Ar⁺ ion cleaning at 2 kV. The deposition processes were performed in DC plasma (U= (1400- 1800)V and I= 75mA) at Ar residual pressure of 4.10⁻²Torr. The nitrogen (99,995 % pure N₂) gas is introduced in the reaction chamber through a needle valve. The specimens E_S1 and E_N3 are deposited at about 0.9 nm/s while E_4 at 2 nm/s, respectively.

Thin films were characterized by ellipsometry, XRD, Raman, IR and XP spectroscopy. The ellipsometry measurements were performed using J.A. Woollam Co., Inc. M2000D rotating compensator spectroscopic ellipsometer with a CCD spectrometer with wavelength range from 193 to 1000 nm. Experimental data for psi and delta were acquired at angles of incidence of 55, 60, 65, 70 and 75 degrees and were modelled using the CompleteEASEWoollam Co., Inc. software. The Raman measurements were carried out in a micro-Raman spectrometer HORIBA Jobin Yvon Labram HR 800 Visible with a He-Ne (633 nm) laser. The laser beam with 0.5 mW power was focused on a spot of about 1 μ m in diameter on the studied surfaces, the spectral resolution being 0.5 cm⁻¹ or better. The X-ray powder diffraction patterns taken from {001} plane for phase identification were recorded in the angle range 2 θ = 24°– 61° (about <011> at $\varphi=0^\circ$ as well as at $\varphi=90^\circ$) on a Philips PW 1050 diffractometer, equipped with a Cu K α tube at temperature of 21°C. A step-scan mode at steps of 0.05°(2 θ) with a counting time of 1 s/step was used for the XRD data collection. The X-ray Photoelectron spectra were obtained using non-monochromatized Al K α (1486.6 eV) radiation in a VG ESCALAB MK II electron spectrometer under base pressure of 1x10⁻⁸ Pa. The spectrometer resolution was calculated from the Ag3d_{5/2} line with the analyzer transmission energy of 20 eV. The full width at half maximum (FWHM) of this line is 1 eV. The spectrometer was calibrated against the Au4f_{7/2} line (84.0 eV) and the samples' charging was estimated from C1s (285 eV) spectra from natural hydrocarbon contaminations on the surface. The accuracy of the BE measured was 0.2 eV. The photoelectron spectra of C1s, O1s, Fe2p, Ni2p as well as CKVV Auger line of carbon films deposited on different substrates were recorded and corrected by subtracting a Shirley-type background and quantified using the peak area and Scofield's photoionization cross-sections. The IR spectra were recorded using a Bruker VERTEX 70 System. The signal was averaged over 64 scans in the spectral range 600-6000cm⁻¹. The spatial resolution was 4 cm⁻¹.

3. Results and discussion

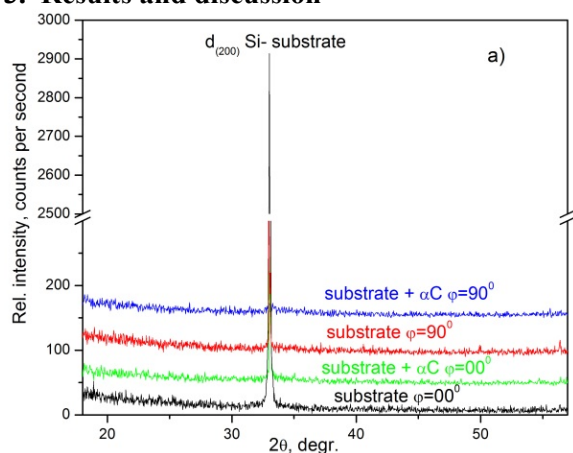


Figure 1 a) XRD pattern of the Si-substrate (black and red traces) as well as the E_4 (green and blue traces) specimens.

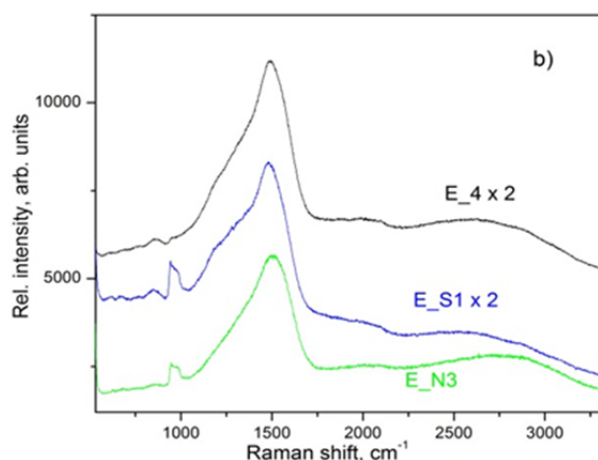


Figure 1 b) Raman spectra of E_4, E_S1 and E_N3 specimens.

The XRD patterns of E_4 specimen (before and after the deposition process) show absence of long range ordering in the carbon layer and only Si (002) reflection appears in the figure 1a). The XRD patterns of E_N3 and E_S1 specimens are not shown here as they are very similar to those of E_4. The Raman spectrum of the specimens E_4, E_N3 and E_S1 (figure 1b) completely coincide with those of hydrogenated amorphous carbon: it is dominated by a broad feature situated at about 1450 cm⁻¹[8].

The IR absorption spectra (figure 2) consist of several weak absorption bands indicated by consequent numbers from 1 to 6, which should be ascribed as follows: 1 and 2- are due to mono-substituted benzene (CH₃-C₆H₅)[9]; 3 and 4- most probably are due to sp³ C-H stretching in aliphatic(-CH₂-..-CH₂-) chains [10]; 5- is the asymmetric vibration ν₃ of [SiO₄]²⁻ group [11] and 6- alkyl-substituted ether (RA-O-RA) species[9].

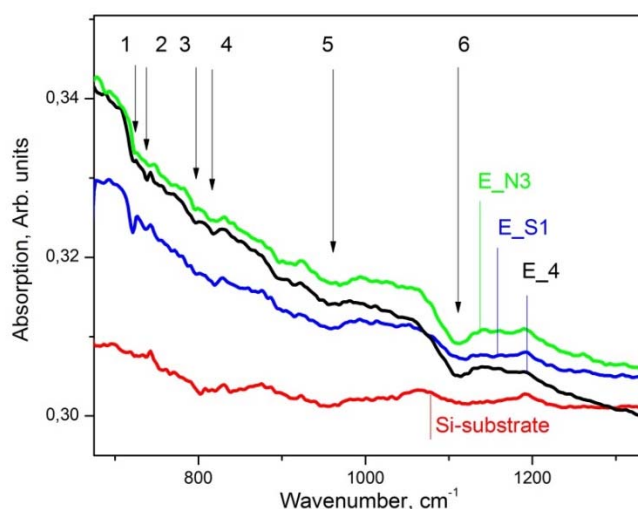


Figure 2. IR absorption spectra of the Si- substrate, E_4, E_N3 and E_S1 specimens.

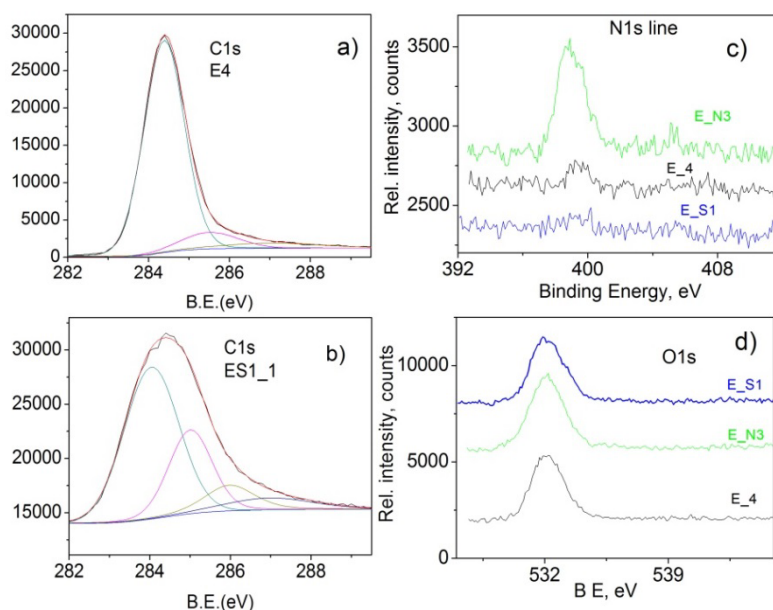


Figure 3. XPS results of E_4 and E_S1 specimens: **a)** and **b)** panels represent C1s lines; **c)** shows N1s lines and **d)** shows O1s lines.

The C1s spectrum of amorphous carbon films (figures 3a and b) is dominated by a single peak at 284.2 eV (corresponding to sp^2 hybridized carbon) and a second peak at the higher binding energy side in the spectra having binding energy at around 284.9 eV (corresponding to sp^3 hybridized carbon) [12,13]. The deconvolutions of 1s carbon spectra gave us possibility to calculate the sp^3/sp^2 ratio and to extract additional information about the carbon to carbon bonds as well as the carbon to oxygen bonds. N1s lines (figure. 3c) pointed to a different concentrations and forms of doping nitrogen: the specimens E_4 and E_S1 contain smaller quantities of nitrogen and the N1s line appears at about 400 eV therefore, it could be ascribed to pyrrolic nitrogen (C_4H_4NH). We associate the last small peak at the higher binding energy side in the N1s spectrum with existence of NO_2 (adsorbed species). The N1s line of E_N3 specimen is very complex but it seems that it contains pyridone nitrogen ($C_5H_4NH(O)$) predominantly. The O1s lines (figure 3d) indicated that the oxygen in the carbon layer of E_4 specimen is below 3 at. % as we observed oxygen as a part of SiO_2 interlayer. The E_S1 and E_N3 carbon layers contain about 3.5 and 2 at. % oxygen, respectively.

For the samples (E_4, E_S1 and E_N3) we detected silicon in none fully oxidation states (the XPS are not shown here). At the same time for the samples ES1 and E_N3 we observed the presence of silicon in SiO_2 . The presence or absence of silicon in the investigated by us highly tetrahedral amorphous carbon films is due to a different thickness of the deposited films as well as due to the used deposition method. The XPS results are summarized in table 1.

Table 1. Summarized results for the layers configuration and thickness as well as for their phase composition obtained by XPS and ellipsometry studies.

Experiment	Fraction sp^3/sp^2 C	C,at%	O,at%	N,at%	Layer configuration	
					Thickness, nm	
					SiO_2	ta-C:H
E_4	0.1	93.56	5.95	0.42	320.9	138.4
E_N3	0.55	90.19	8.48	1.33	427.5	26.2
E_S1	0.42	93.65	6.03	0.23	2.89	114.2

The measured ellipsometry spectra were fit in two different ways depending on the properties of the films:

-samples E_N3 and E_4 (the ta-C:H and α -C:H layers are deposited on a 300-400 nm thick thermal SiO_2 layer): a 3-layer model was used to represent the sample, consisting of a silicon substrate, a thermal silicon oxide layer (as a 1st layer), an α -C layer as a second layer and a roughness layer as a third layer. Each layer is determined by its thickness and dielectric constants. For the silicon substrate and the thermal silicon oxide layer we used the models Si_JAW and SiO_2_JAW from the CompleteEASE data analysis software library. The top α -C layer was first represented as a b-spline layer with starting material Graphite_o_Palic_nk from CompleteEASE data analysis software library. The thickness of the thick thermal SiO_2 layer was determined by adjusting the number of the psi and delta oscillations and their amplitude was adjusted by varying the thickness of the alpha-C layer deposited on the top. This method is known as “interference enhancement method” and allows a unique determination of both the thickness and the optical constants of thin absorbing films on opaque substrates from VASE data [14]. The dielectric function of the alpha-C layer described by the b-spline model was then parametrised using the General oscillator (Gen-Osc) model including one Cody-Lorentz and one Gaussian oscillator. The Gen-Osc parametrization was used to reduce the number of the unknown fit parameters as well as to ensure Kramers-Kronig consistent optical properties [15,16].

-sample E_S1 (the ta-C:H layer is deposited on a 2-4 nm thick native SiO_2): a 3-layer model was used to represent the sample, consisting of a silicon substrate, a silicon native oxide layer (as a 1st layer), an alpha-C layer as a second layer and a roughness layer as a third layer. For the silicon substrate and the native silicon oxide layer we used the models Si_JAW and NTVE_JAW from the CompleteEASE data analysis software library. The thickness of the silicon native oxide layer was determined on a bare substrate before the deposition of the top ta-C:H layer. The layer was then

parametrised using b-spline model to fit the optical constants in the absorbing area. Finally, the dielectric function of the b-spline layer was parametrized using the General oscillator model including one Cody-Lorentz and one Gaussian oscillator.

The roughness layer for all samples is modeled by Bruggeman's EMA (Effective Medium Approximation) of 50% voids and 50% bulk material [16].

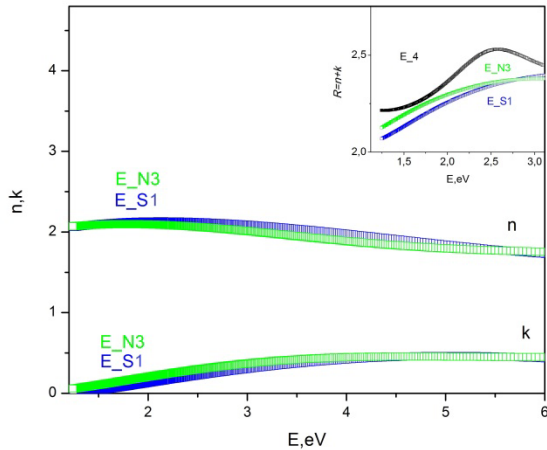


Figure 4. Optical parameters: R-refractive index, n- refraction coefficient and k- extinction coefficient obtained from the ellipsometry measurements.

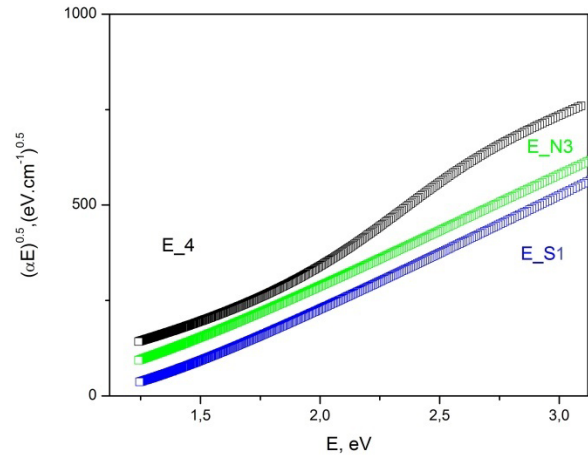


Figure 5. Calculated energy of indirect interbandtransitions (by Tauc relation: $\alpha E = A(E - E_g)^{0.5}$) [13] in E_4, E_S1 and E_N3.

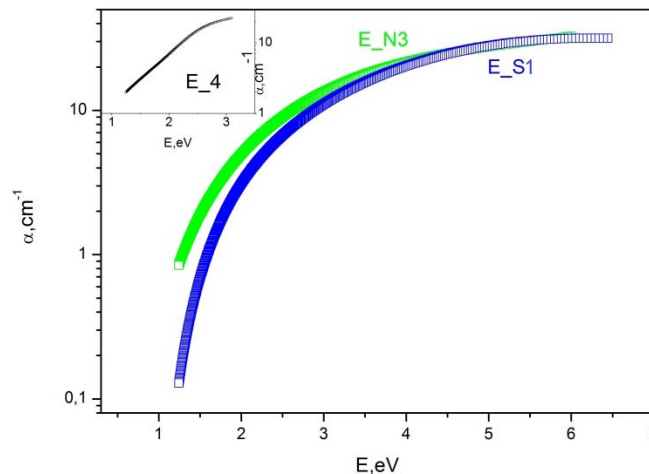


Figure 6. Energy of the indirect interband transitions in E_S1 and S_N3 specimens and the defect Urbach-tail states (the inset) in E_4 specimen.

The spectral dependence of the basic optical parameters of the films (R - refractive index $R=n+k$, n - refraction coefficient and k - extinction coefficient) determined by that way are plot in figure 4. Furthermore, the absorption coefficient (α), the energy of indirect interbandtransition- E_g (shown in figure 5 and 6 as well as the excitation energy of the defect Urbach tail states- E_u (shown in the inset of figure 6) were calculated from these datasets by relations [17, 18, 19]:

$$\alpha = 4\pi k/\lambda \tag{1}$$

$$\alpha E = A(E - E_g)^{0.5} \tag{2}$$

$$\alpha(E) = \alpha_0 \exp((E - E_g)/E_u) \tag{3}$$

Then, the energy of indirect interband transition in specimens E_N3 and E_S1 is about 1.07 and 1.27 eV, respectively- see figures 5 and 6. The energy of defect driven Urbach-tail states in specimen E_4 is about 0.93 eV- see the inset of figure 6. We did not observe tail states in specimens E_N3 and E_S2. This fact can be related to the low deposition rate and minimized disorder in the deposited films. It seems also that the nitrogen occupies different positions in the carbon framework depending on the dominating hybridization of carbon, thus resulting in different energy levels in the bandgap and charge transport properties of the doped films.

4. Conclusions

We deposited successfully nitrogen doped ta-C:H and α C:H layers with thicknesses (20-150 nm) and nitrogen concentrations from 0.2 to 1.5 at.%. The mole fraction of sp^2 to sp^3 hybridized carbon content could be varied by the DC- plasma voltage in the range 90/10 to 60/40 at. %. The layers are amorphous and contain predominantly C_6H_6 ; $CH_3-C_6H_5$ and sp^3 C aliphatic(-CH₂-...-CH₂-) species. The energy gap of indirect transitions in E_N3 and E_S1 layers is about 1.07 eV and 1.27 eV, respectively. The excitation energy of the defect Urbach tail states is about 0.93 eV in E_4 specimen. The lowered deposition rate from 2nm/s to below 1 nm/s decreases disorder and related tail states.

Acknowledgements:

The authors gratefully acknowledge the support from INERA "Research and Innovation Capacity Strengthening of ISSP BAS in Multifunctional Nanostructures" Project as well MPNS COST ACTION MP -1204.

References

- [1] Tinchev S, Nikolova R, Dyulgerska J, Danev G and Babeva Tz 2005 *Solar Energy Materials Solar Cells* **86** 421
- [2] Robertson J and Davis C 1995 *Diamond Rel. Mater.* **4** 441
- [3] Robertson J 2002 *Mater. Sci. Engineer. R* **37** 129
- [4] Koidl P, Wild C, Dischler B, Wagner J, Ramsteiner M 1990 *Materials Science Forum* **52-53** 41
- [5] Kalish R, Amir O, Brener R, Spits R A and Derry T E 1991 *Appl. Phys. A* **52** 48
- [6] Han H X and Feldman B J 1988 *Solid State Commun.* **65** 921
- [7] Kaufman J H, Metin S and Saperstein D D 1989 *Phys. Rev. B* **39** 13053
- [8] Ferrari A and Robertson J 2004 *Phil. Trans. R. Soc. Lond. A* **362** 2477
- [9] *Interpretation of Infrared Spectra, A Practical Approach by John Coates in Encyclopedia of Analytical Chemistry* (John Wiley & Sons Ltd, Chichester 2000) pp 10815-10837
- [10] Chevalier J, Bergeron J and Dao L 1992 *Macromolecules* **25** 3325
- [11] Nakamoto K 1989 *Infrared and Raman spectra in Inorganic and Coordination Compounds* (New York: John Willey & Sons.) IV 138
- [12] Lascovich J, Giorgi R and Scaglione S 1991 *Appl. Surf. Sci.* **47** 17
- [13] Díaz J, Paolicelli G, Ferrer S and Comin F 1996 *Phys. Rev. B* **54** 8064
- [14] McGahan W, Johns B and Woollam J 1993 *Thin Solid Films* **234** 443
- [15] Hilfiker J, Singh N, Tiwald T, Convey D, Smith S, Baker J and Tompkins H 2008 *Thin Solid Films* **516** 7979
- [16] *CompleteEASE*[®] Software Manual (Lincoln: J.A. Woollam Co.) USA
- [17] Dresselhaus M 2001 *Solid State Physics, p.II, Optical Properties of Solids*, p.36
- [18] Tauc J, Grigorovici R and Vancu A 1966 *Phys. Status Solidi* **15** 627
- [19] Urbach F 1953 *Phys. Rev.* **92** 1324